Transactions of the Materials Research Society of Japan 29[6] 2675-2678 (2004)

Novel Techniques of Hydroxyapatite Coating on Titanium Utilizing Hydrothermal Hot-pressing

Takamasa Onoki, Kazuyuki Hosoi* and Toshiyuki Hashida
Fracture Research Institute, Tohoku University, 01 Aoba, Aramaki, Aoba-ku, Sendai, 980-8579, Japan.
Fax: 81-22-217-4311, e-mail: onoki@rift.mech.tohoku.ac.jp
*Shiraishi Kogyo Kaisha Ltd., 4-78 Motohamacho, Amagasaki, 660-0085, Japan.
Fax: 81-6-6417-4832, e-mail: hosoi@kogyo.shiraishi.co.jp

Solidification of hydroxyapatite (HA) and its coating on titanium (Ti) rod was achieved simultaneously by utilizing a hydrothermal hot-pressing (HHP) method at the low temperature as low as 150℃. A mixture of calcium hydrogen phosphate dehydrate (DCPD) and calcium hydroxide was used as a starting powder material for HA coating. The powder mixture and Ti rod was placed in an autoclave for HHP treatment. Some Ti rods were treated with alkali solution before HHP treatment.

Pull-out tests were conducted to obtain an estimate of the interfacial property or the HA/Ti interface. The shear fracture strength obtained from the pull-out tests was approximately 3.0MPa. In post-test observations after fracture tests, HA ceramics remained on Ti rod. It could be demonstrated that the fracture occurred into the HA ceramics, not into the HA/Ti interface. Especially, the alkali solution treatment could improve the fracture properties of the interface between HA ceramics coating and Ti rod.

Key words: Alkali solution treatment, Pull out test

1. INTRODUCTION

Titanium (Ti) and its alloy are widely used as orthopedic and dental implant materials because of their high mechanical strength, low modulus and good corrosion resistance.[1] Traditionally, Ti and its alloys have been reported as bioinert. When embedded in the human body, a fibrous tissue capsules the implant isolating from the surrounding bone forms.

Some bioactive ceramics such as hydroxyapatite (HA), bioglass and glass ceramics can directly bond to living bone when used as bone replacement materials.[2] HA ceramics are biomaterials which have been extensively developed recently.[3,4] In the traditional method for solidifying HA, HA powder was sintered at high temperatures over 1000 ° C.[5] The mechanical properties of bulk HA only allow applications for small non-loaded structure.[6] The possibility of depositing it into films has permitted to exploit its bioactive properties in structural prostheses such as teeth root, hip, knee and shoulder joint replacement. Therefore, HA is also used as a coating material for those prostheses surface in order to prepare bioactive layers on titanium and its alloys.[7] The HA surface improves the fixation of implants by the growth of bone into the coating, forming a mechanical interlock. A plasma spraying technique has been frequently employed for the coating process of HA.[8, 9] However, this high temperature method results in some of significant problems like a poor coating-substrate adherence[10], lack of uniformity of the coating in terms of morphology and crystallinity[11, 12], that affect the long-term performance and lifetime of the implants. Other techniques are also available such as: sintering, chemical vapor deposition, sol-gel deposition, ion implanting, laser deposition and electrochemical process like electrophoretic deposition, electrocrystallization and anode oxidation. Despite of all the investigations carried out, the produced coatings can suffer from at least one of the following problems: Lack of coating adherence to the substrate, poor structure integrity and non-stoichiometric composition of the coatings.[13]

HA is the most thermodynamically stable phase among the calcium phosphate compounds. Other calcium phosphate compounds are readily transformed into HA in the presence of some solutions at relatively low temperatures (below 100° C). The hydrothermal reaction of calcium hydrogen phosphate dihydrate ($CaHPO_4 \cdot 2H_2O$; DCPD) to HA is relatively easy when it occurs in a solution.[14-16] Moreover, the transformation into HA is accelerated by the supply of Ca^{2+} and PO_4^{3-} at the stoichiometric ratio of Ca/P=1.67 in HA. For example, the chemical reaction of DCPD and calcium hydroxide ($Ca(OH)_2$) occurs in a liquid phase as follows:

$$6CaHPO_4 \cdot 2H_2O + 4Ca(OH)_2 \rightarrow Ca_{10}(PO_4)_6(OH)_2 + 18H_2O \quad \cdots (1)$$

This chemical reaction progresses at low temperatures (typically less than 80° C).[17] The only products of the above reaction are HA and water.

Hydrothermal hot-pressing (HHP) method is a possible processing route for producing a ceramic body at relatively low temperatures.[18, 19] The compression of samples under hydrothermal conditions accelerates

densification of inorganic materials. It is known that the water of crystallization in DCPD is slowly lost below 100° C. If the released water can be utilized as a reaction solvent during the HHP treatment, it is to be expected that the joining HA to metal can be achieved simultaneously under the hydrothermal condition, in addition to the synthesis and solidification of HA.[20]

This paper describes a new technique of coating HA ceramics to Ti by using the HHP method.

2. EXPERIMENTAL PROCEDURE

2.1 Sample preparation

A commercially available pure Ti rod (99.5%; Nilaco, Japan), 1.5mm in diameter, was used in this experiment. The Ti rod was cut into a length of approximately 18mm. The rods were cleaned in deionized water and acetone by using an ultrasonic cleaner. Ti surfaces were finished using 1500# emery paper. After the surface finish with emery paper, the titanium rods were washed again by deionized water, and then dried in air. Recently, it has been reported that if the Ti and its alloys surface is treated with sodium hydroxide (NaOH) solution it obtains the ability of joining HA directly by a biomimetic method.[21] In order to investigate the effects of alkali solution treatment, the Ti rods were treated with alkali solution (5*M* NaOH). The conditions of a NaOH solution hydrothermal treatment were conducted at 150°C for 2h. After the hydrothermal treatments, the Ti rods were washed by deionized water, and then dried in air. 2 kinds of Ti rods were prepared, whether with the alkali solution treatment or without the treatment.

DCPD used as a starting powder was prepared by mixing 1.0*M* calcium nitrate solution (99.0%; $Ca(NO)_3 \cdot 4H_2O$, KANTO CHEMICAL CO., INC., Japan) and 1.0*M* diammonium hydrogen phosphate solution (98.5%; $(NH_4)_2HPO_4$; KANTO CHEMICAL CO., INC., Japan). The mixing was carried out at a room temperature (approximately 20° C). In order to control the value of pH, acetic acid and ammonia solution were added. The precipitate from the mixture was filtered and washed with deionized water and acetone. The washed filter cake was oven-dried at 50° C for 24h, and then the dried cake was ground to a powder. The synthetic DCPD and calcium hydroxide (95.0%; $Ca(OH)_2$; KANTO CHEMICAL CO., INC., Japan) were mixed in a mortar for 30min with a Ca/P ratio of 1.67.

2.2 Autoclave for HHP treatment

The autoclave made of stainless steel (SUS304) has a pistons-cylinder structure with an inside diameter of 20mm, as shown in Fig.1. The pistons possess escape space for hydrothermal solution squeezed from the sample, and this space regulates the appropriate hydrothermal conditions in the sample. A grand packing of polytetrafluoroethylene (PTFE) is placed between a cast rod and push rod. The PTFE was used to prevent leakage of the hydrothermal solutions.

A pressure of 40MPa was applied to the sample through the push rods from the top and bottom at a room temperature. After the initial loading the autoclave was heated up to 150° C at heating rate of 10° C/min, and then the temperature was kept constant for 3hours. The autoclave was heated with a sheath-type heater. The axial pressure was kept at 40MPa during the HHP treatment. After the HHP treatment, the autoclave was naturally cooled to a room temperature, and the sample

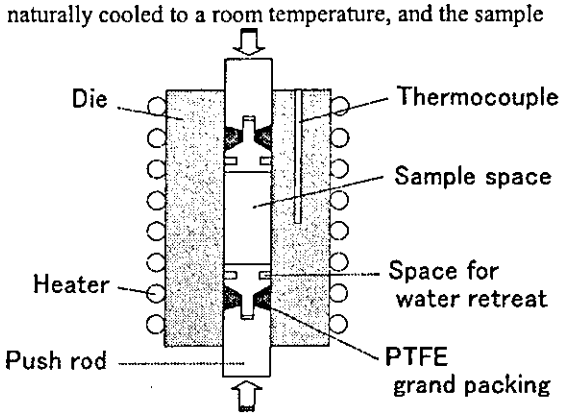

Fig.1 Schematic illustration of the autoclave for Hydrothermal Hot-pressing method

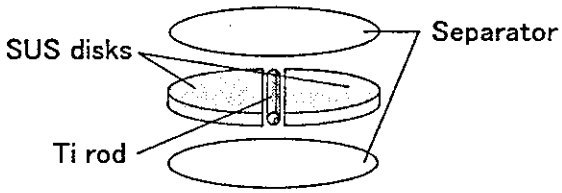

Fig.2 Schematic illustration of the configuration around the Ti rod.

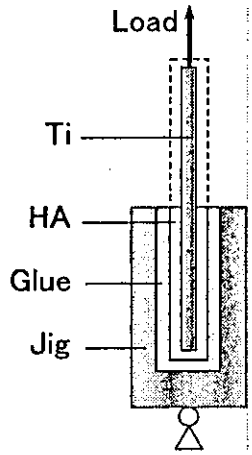

Fig.3 Schematic illustration of the pull out test in a cross section view.

removed from the autoclave.

A Ti rod and the powder mixture of DCPD and $Ca(OH)_2$ were placed into the middle of the autoclave simultaneously. The configuration is shown in Fig.2. The mixed powder of DCPD and $Ca(OH)_2$ were located between separators. The separators were made of PTFE membranes. A Ti rod was located between 2 pieces of stainless steel (SUS304) disks as shown in Fig.2. SUS disks which could not be bonded to HA ceramics by

HHP method were made semicircle shape in order to keep appropriate space for a Ti rod and the HA starting powder. Thickness of the SUS disks was 2mm. Upper and lower sides spaces of separators were filled with pressure media which was aluminum oxide powder (3.0μm; BUEHLER LTD., USA). The separators were used to reduce the mixing of aluminum oxide powder and HA starting powder.

2.3 Coating Strength evaluation

Pull out tests were conducted in order to evaluate bonding strength of the HA ceramics coating. The detail of pull out tests is drawn in Fig.3. The HA coated samples were fixed to the test jigs by epoxy resin (Araldite; CHIBA-GEIGY). And then the part of HA coating without attaching to the jig was removed with a knife and a grinder. The specimens were loaded at a cross-head speed of 0.5mm/min until the Ti rods were pulled out entirely. Fracture behaviors were observed and the stress-displacement curves were measured.

3. RESULTS AND DISCUSSION

As demonstrated in Fig.4, the HA ceramics could be coated to the all surface of Ti rods at the low temperature of 150°C using the above-mentioned HHP treatment.

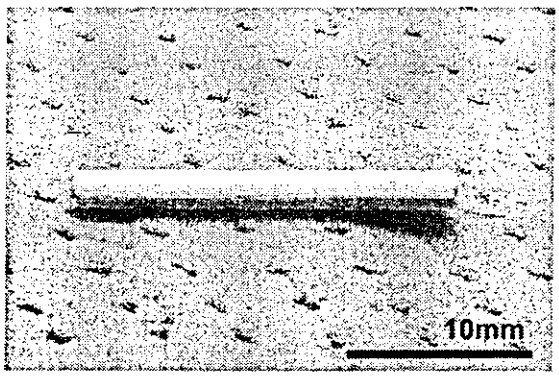

Fig.4 Photographs of the sample of HA coating on Ti rod.

Fig.5 shows photographs of the specimens after pull out tests. The left parts of the specimens were fixed onto the test jigs. The photograph of Fig.5(a) and (b) are the specimens without the alkali solution treatment and with treatment respectively. As shown in Fig.5(b), it can be seen that HA coating remains on the Ti rod in contrast with Fig.5(a). It can be noted that the fracture occurs not at the HA/Ti interface, but in the HA. This observation suggests that the fracture toughness of the HA/Ti interface is close to or higher than that of the HA ceramics only.

The load-displacement curves in pull out tests are shown in Fig.6(a) and (b) without the alkali solution treatment and with the treatment respectively. It is seen in Fig.6(a) that the load decreases approximately linearly after the peak as the displacement is increased. This observation in conjunction with Fig.5(a) suggest that the interface between the HA and Ti rod is held just by interfacial friction and no significant chemical bond is expected for the interface without the alkali solution treatment.

On the other hand, the load-displacement curve of the specimen treated with the alkali solution, as shown in Fig.6(b), shows the different tendency where the load temporarily increases after the peak. The results of Fig.6(b) and fracture surface observation imply that there is a chemical bond between the HA and Ti rod. As described previously, the crack propagation took place in the HA, not along the interface. The deviation and kinking of the crack path from the interface may induce an additional frictional resistance to the crack propagation in the pull-out test. This may explain the second peak in the load-displacement curve shows in Fig.6(b).

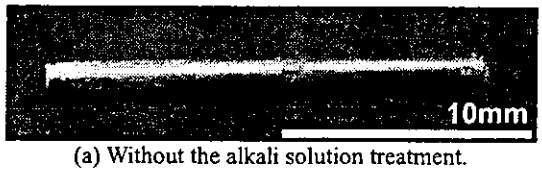

(a) Without the alkali solution treatment.

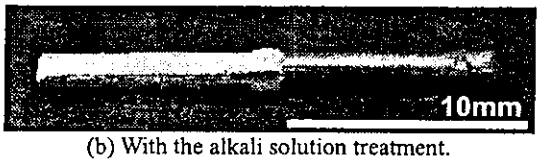

(b) With the alkali solution treatment.

Fig.5 photographs of the samples after pull out tests.

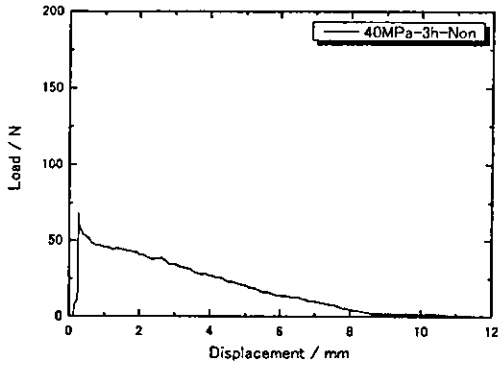

(a) Without the alkali solution treatment.

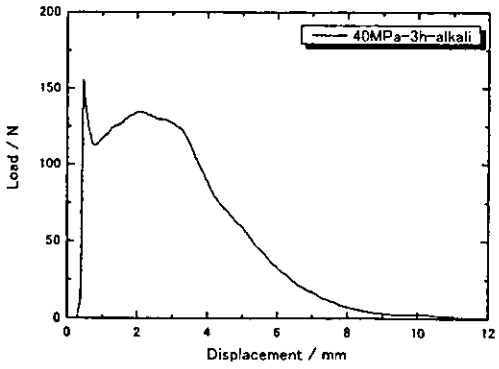

(b) With the alkali solution treatment.

Fig.6 The stress-displacement curves of pull out tests.

In order to evaluate the effects of the alkali solution treatment quantitatively, the shear strength and fracture energy were calculated from the results of pull out tests, and are plotted in Fig.7. The shear strength, τ is computed based on the following equation:

$$\tau = \frac{P_{max}}{\pi dL} \quad \cdots (2)$$

where d is the diameter of Ti rods(1.5mm), L is the fixed length of Ti rods, P is load, P_{max} is the maximum value of P. τ is estimated to be 1.5MPa for the specimen without the alkali solution treatment and 3.0MPa for the treated specimen, respectively. The averaged shear strength over the embedment length L maybe taken as a fracture property of initiation. The alkali solution treatment improved the initiation resistance two times more than the non-treated condition. The fracture energy G is calculated using the following equation:

$$G = \frac{A}{\pi dL} \quad \left(A = \int_0^x P dx \right) \cdots (3)$$

where x is the displacement of cross-head. G is estimated 4.0Nmm^{-1} for the specimen without the alkali solution treatment and 11.9Nmm^{-1} for the treated specimen, respectively. It was shown three times improvement. It is seen that the alkali solution treatment on Ti rods allows us to improve the interfacial fracture property.

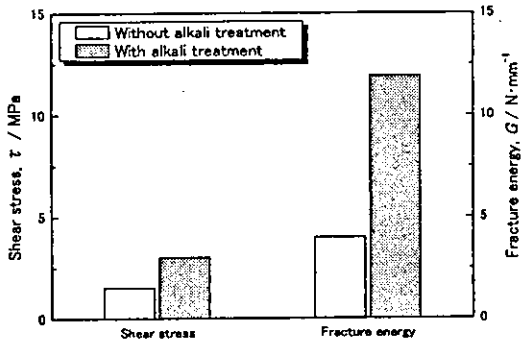

Fig.7 Shear fracture stress and fracture energy calculated from pull out tests.

While further development is needed to improve the fracture property of the solidified HA, the HHP treatment may have the advantage over the plasma-spraying technique in the preparation of thermodynamically stable HA. The above results demonstrate the usefulness of the HHP method for coating HA on Ti in order to produce a bioactive layer in biomaterials.

4. CONCLUSIONS

In this paper, it was demonstrated that HA ceramics could be coated to Ti rods using a hydrothermal hot-pressing method at the low temperature as well as 150° C. Especially for the sample treated with alkali solution, the pull out tests conducted on the HA coating sample revealed that fracture occurred not along the interface but in the HA ceramics. The fracture property of the HA/Ti interface was also suggested to be close to or higher than that of the HA ceramics. Investigation of the bonding mechanism and in vivo tests of the HA coating samples are in progress.

ACKNOWLEDGEMENT

This study was supported in part by the Japan Ministry of Health, Labour and Welfare under Grants-in Aid for Research on Advanced Medical Technology. Author T.O. was supported by research fellowship of the Japan society for the promotion of science for young scientists.

5. REFERENCES

(1) M. Long and H. J. Rack, *Biomaterials* 19, 1621 (1998).
(2) L. L. Hench, *J. Am. Ceram. Soc.* 81, 1705 (1998).
(3) M. Jarcho, J. F. Kay, K. I. Gummaer, R. H. Doremus and H. P. Drobeck, *J. Bioengng.* 1, 79 (1977).
(4) H. Aoki, "In Medical Applications of Hydroxyapatite" Ishiyaku Euro-America, Tokyo, Japan, (1994), pp. 133-154.
(5) J. G. J. Peelen, B. V. Rejda and K. De Groot, *Ceramurgia Int.* 4, 71 (1978).
(6) L. L. Hench, *J. Am. Ceram. Soc.* 74, 1487 (1991).
(7) P. Ducheyne, L. L. Hench, A. Kagan, M. Martens, A. Burssens and J. C. Mulier, *J. Biomed. Mater. Res.* 14, 225 (1980).
(8) S. R. Radin and P. Ducheyne, *J. Mater. Sci. Mater. Med.* 3, 33 (1992).
(9) K. De Groot, R. Geesink, C. P. A. T. Klein and P. Serekian, *J. Biomed. Mater. Res.* 21, 1375 (1987).
(10) X. Zheng, M. Huang and C. Ding, *Biomaterials* 21, 841 (2000)
(11) H. C. Gledhill, I.G Turner and C. Doyle, *Biomaterials* 22,695 (2001).
(12) F. Fazan and P. M. Marquis, *J. Mater. Sci. Mater. Med.* 11, 787 (2000).
(13) K. A. Thomas, *Orthopaedics* 17, 267 (1994).
(14) E. E. Berry, *J. Inorg. Nucl. Chem.* 29, 317 (1967).
(15) A. Atkinson, P. A. Bradford and I. P. Selemes, *J. Appl. Chem. Biotechnol.* 23, 517 (1978).
(16) H. Monma and T. Kamiya, *J. Mater. Sci.* 22, 4247 (1987).
(17) T. Matsuno and M. Koishi, *Shikizai* 65, 238 (1992).
(18) N. Yamasaki, K. Yanagisawa, M. Nishioka and S. Kanahara, *J. Mater. Sci. Lett.* 5, 355 (1986).
(19) N. Yamasaki, T. Kai, M. Nishioka, K. Yanagisawa and K. Ioku, *J. Mater. Sci. Lett.* 9, 1150 (1990).
(20) K. Hosoi, T. Hashida, H. Takahashi, N. Yamasaki and T. Korenaga, *J. Am. Ceram. Soc.* 79, 2771 (1996).
(21) H. M. Kim, F. Miyaji, T. Kokubo and T. Nakamura: *J. Biomed. Mater. Res.*, 32, 409 (1996).

(Received October 13, 2003; Accepted February 9, 2004)

Transactions of the Materials Research Society of Japan 29[6] 2929-2932 (2004)

GD-OES Analysis of the Interface between Titanium and Hydroxyapatite Ceramics Produced by Hydrothermal Hot-pressing Method

Takamasa Onoki, Kazuyuki Hosoi* and Toshiyuki Hashida
Fracture Research Institute, Tohoku University, 01 Aoba, Aramaki, Aoba-ku, Sendai, 980-8579, Japan.
Fax: 81-22-217-4311, e-mail: onoki@rift.mech.tohoku.ac.jp
*Shiraishi Kogyo Kaisha Ltd., 4-78 Motohamacho, Amagasaki, 660-0085, Japan.
Fax: 81-6-6417-4832, e-mail: hosoi@kogyo.shiraishi.co.jp

Solidification of hydroxyapatite (HA) and its bonding with titanium (Ti) was achieved simultaneously by using a hydrothermal hot-pressing method at the low temperature as low as 150℃. A mixture of calcium hydrogen phosphate dehydrate(DCPD) and calcium hydroxide was used as a starting powder material for solidifying HA. 3-point bending tests were conducted to obtain an estimate of the fracture toughness for the HA/Ti interface as well as for the HA ceramics only. The fracture toughness tests showed that the induced crack from the pre-crack tip deviated from the HA/Ti interface and propagated into the HA. The fracture toughness determined on the HA/Ti specimen was closed to that of the HA ceramics only (K_c=0.30 MPam$^{1/2}$).

Depth profile of the chemical composition determined by glow discharge optical emission spectroscopy (GD-OES) method indicated that the bonding of HA and Ti was achieved though the formation of a reaction layer at the HA/Ti interface. The thickness of the reaction layer was estimated to be approximately 1μm. It seemed that this reaction layer provided the bonding HA/Ti for absorbing the misfit between HA and Ti.
Key words: Hydrothermal hot-pressing, Bonding, Diffusion

1. INTRODUCTION

Titanium (Ti) and its alloy are widely used as orthopedic and dental implant materials because of their high mechanical strength, low modulus and good corrosion resistance.[1] Traditionally, Ti and its alloys have been reported as bioinert. When embedded in the human body, a fibrous tissue capsules the implant isolating from the surrounding bone forms.

Some bioactive ceramics such as HA, bioglass and glass ceramics can directly bond to living bone when used as bone replacement materials.[2] HA ceramics are biomaterials which have been extensively developed recently.[3,4] In the traditional method for solidifying HA, HA powder was sintered at high temperatures over 1000°C.[5] The mechanical properties of bulk HA only allow applications for small non-loaded structure.[6] The possibility of depositing it into films has permitted to exploit its bioactive properties in structural prostheses such as teeth root, hip, knee and shoulder joint replacement. Therefore, HA is also used as a coating material for those prostheses surface in order to prepare bioactive layers on titanium and its alloys.[7] The HA surface improves the fixation of implants by the growth of bone into the coating, forming a mechanical interlock. A plasma spraying technique has been frequently employed for the coating process of HA.[8, 9] However, this high temperature method results in some of significant problems like a poor coating-substrate adherence[10], lack of uniformity of the coating in terms of morphology and crystallinity[11, 12], that affect the long-term performance and lifetime of the implants. Other techniques are also available such as: sintering, chemical vapor deposition, sol-gel deposition, ion implanting, laser deposition and electrochemical process like electrophoretic deposition, electrocrystallization and anode oxidation. Despite of all the investigations carried out, the produced coatings can suffer from at least one of the following problems: Lack of coating adherence to the substrate, poor structure integrity and non-stoichiometric composition of the coatings.[13]

HA is the most thermodynamically stable phase among the calcium phosphate compounds. Other calcium phosphate compounds are readily transformed into HA in the presence of some solutions at relatively low temperatures (below 100°C). The hydrothermal reaction of calcium hydrogen phosphate dihydrate ($CaHPO_4 \cdot 2H_2O$; DCPD) to HA is relatively easy when it occurs in a solution.[14-16] Moreover, the transformation into HA is accelerated by the supply of Ca^{2+} and PO_4^{3-} at the stoichiometric ratio of Ca/P=1.67 in HA. For example, the chemical reaction of DCPD and calcium hydroxide ($Ca(OH)_2$) occurs in a liquid phase as follows:

$$6CaHPO_4 \cdot 2H_2O + 4Ca(OH)_2 \rightarrow Ca_{10}(PO_4)_6(OH)_2 + 18H_2O \quad (1)$$

This chemical reaction progresses at low temperatures (typically less than 80°C).[17] The only products of the above reaction are HA and water.

Hydrothermal hot-pressing (HHP) method is a

possible processing route for producing a ceramic body at relatively low temperatures[18, 19]. The compression of samples under hydrothermal conditions accelerates densification of inorganic materials. It is known that the water of crystallization in DCPD is slowly lost below 100° C. If the released water can be utilized as a reaction solvent during the HHP treatment, it is to be expected that the joining HA to metal can be achieved simultaneously under the hydrothermal condition, in addition to the synthesis and solidification of HA.[20]

This paper describes a new technique of bonding HA ceramics and Ti by using the HHP method and the interface properties between HA ceramics and Ti.

2. EXPERIMENNTAL PROCEDURES

2.1 Sample preparetion

Firstly DCPD used as a starting powder was prepared by mixing 1.0*M* calcium nitrate solution ($Ca(NO)_3 \cdot 4H_2O$; KANTO CHEMICAL CO., INC., 99.0%) and 1.0*M* diammonium hydrogen phosphate solution ($(NH_4)_2HPO_4$; KANTO CHEMICAL CO., INC., 98.5%). The mixing was carried out at *a* room temperature (approximately 20℃). In order to control the value of pH, acetic acid and ammonia solution were added fitly. The precipitate from the mixture was filtered and washed with deionized water and acetone. The washed filter cake was oven-dried at 50℃ for 24h, and then the dried cake was ground to a powder.

A commercially available pure Ti rod, 20mm in diameter, was used as a bioinert material. The Ti rod was cut into disks with a thickness of 10mm. And the disks were cleaned in deionized water and acetone by using ultrasonic cleaner. Ti surfaces were treated by two different methods : the Ti surfaces were finished using 1500# emery paper. After emery paper finish, the titanium disks were washed by deionized water, and then dried in air. Synthetic DCPD and calcium hydroxide ($Ca(OH)_2$; KANTO CHEMICAL CO., INC., 95.0%) were mixed in a mortar for 30min with a Ca/P ratio of 1.67. The powder mixture and Ti disks were placed into the middle of the autoclave simultaneously, as shown in Fig.1.

The autoclave which was made of stainless steel (SUS304) has a pistons-cylinder structure with an inside diameter of 20mm in this research. The pistons possess escape space for hydrothermal solution squeezed from the sample, and this space regulates the appropriate hydrothermal conditions in the sample. A grand packing made of polytetrafluoroethylene (PTFE) is fixed between a cast rod and a push rod, and it is deformed by pressure from the top and bottom to prevent leakage of the hydrothermal solutions.

A pressure of 40MPa was applied to the sample through the loading rods from the top and bottom at room temperature. The pressure was kept 40MPa automatically in all stage. After the loading the autoclave was heated up 150℃ at heating rate of 10℃/min, and then the temperature was kept constant for 2hours. The autoclave was heated with a sheath-type heater. The initial axial pressure was kept at 40MPa at initial state of the HHP treatment. After the treatment, the autoclave was cooled to room temperature naturally, and the sample removed from the autoclave.

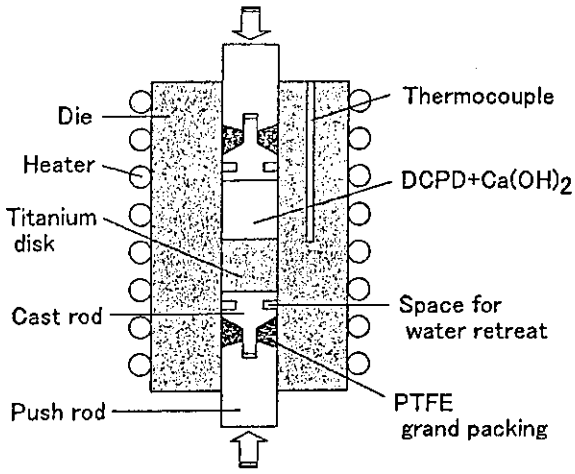

Fig.1 The schematic illustration of the autoclave for Hydrothermal Hot-Pressing(HHP).

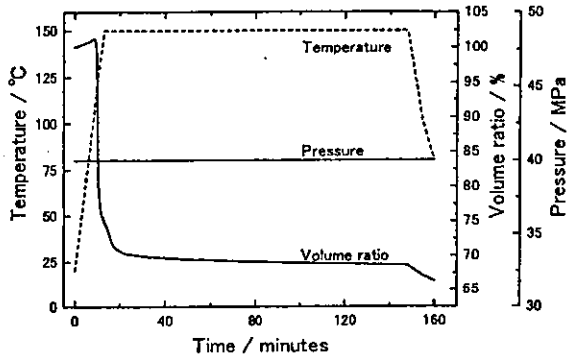

Fig.2 The indication of the temperature, shrinking behavior and pressure during HHP treatment.

The shrinkage behavior of the sample during the HHP treatment was monitored by measuring the relative movement between the two pistons using a displacement gage. The displacement data were used to determine the volume ratio *V* of the sample, defined as follows:

$$V = \frac{h_i - \Delta h}{h_i} \times 100 \qquad (2)$$

where h_i is initial sample height, and Δh is the relative displacement during the heating process.

The typical example of temperature and pressure record is shown in Fig.2, along with volume ratio data. It is seen that the shrinkage started at approximately 90° C. This temperature is close to the dehydration temperature of DCPD. Thus, it is thought that the shrinkage is initiated by the dehydration of DCPD. The shrinkage rate became larger with the increasing temperature, and then the shrinkage rate became smaller. The shrinkage continued during the HHP treatment. The pressure was held at 40MPa constant for the whole period of HHP treatment.

2.2 Evaluation method

3-point bending tests were conducted to obtain an estimate of the fracture toughness for the HA/Ti interface. Core-based specimens were used for the fracture toughness tests and a pre-crack was introduced along the HA/Ti interface of the bonded specimens, following the ISRM suggested method [21]. The stress intensity factor K was used to evaluate of the bonding strength of the HA/Ti. The critical stress intensity factor is used in order to evaluate the fracture toughness for the HA/Ti interface. K is expressed as follows:

$$K = 0.25\left(\frac{S}{D}\right)Y_c'\frac{F}{D^{1.5}} \qquad (3)$$

where D is the diameter of the specimen 20mm, S is supporting span = 3.33D, F is load, Y'_c is dimensionless stress intensity factor. The value of Y'_c is a function of the relative length, a/D. Y'_c was used to calculate the stress intensity factor [21].

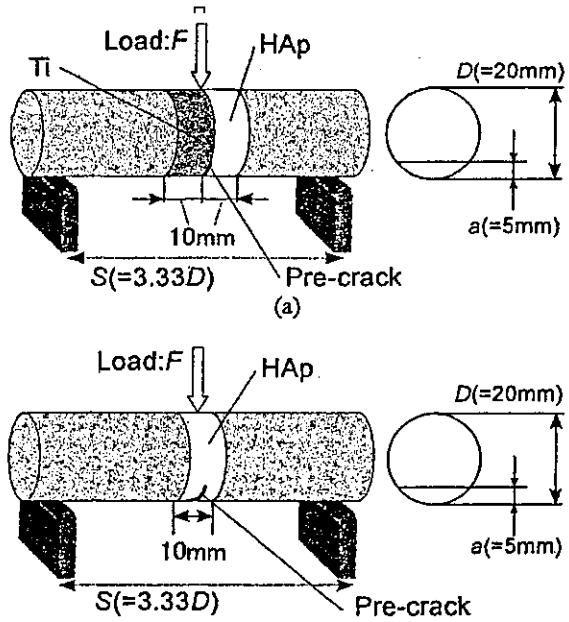

Fig.3 Schematic illustrations of 3-point bending test.

The configuration of the core-based specimen is shown in Fig.3(a) schematically. The steel-rods were attached to HA/Ti body using epoxy resin in order to prepare standard core specimens required for the ISRM suggested method. It should be mention here that the formula given in equation(3) is derived under the assumption of isotropic and uniformed materials. The jointed specimen used in this study for 3-point bending test composed 2 or 3 kinds of materials and is in a homogeneous beam. While exact anisotropic solution is needed for quantitative evaluation of the critical stress intensity factor, the isotropic solution in equation(3) is used to obtain and estimate of the fracture toughness for the HA and HA/Ti in this study. The specimens configurations shown in Fig.3 were used in order to examine the fracture behavior for the HA/Ti bonding body. The pre-crack was induced at the HA/Ti interface. The width of pre-crack was less than 50μm. In case of 3-point bending tests specimens of HA ceramics only, a pre-crack was introduced in the center of HA ceramics as shown in Fig.3(b). The pre-crack was located the center position between two supporting points. The specimens were loaded until a fast fracture took place at a cross-head speed of 1mm/min.

2.3 Interface properties

In order to investigate the construction near the interface between HA ceramics and Ti disk, the bonding bodies were applied to analyses of glow discharge optical emission spectroscopy (GD-OES: JOBIN-YVON HORIBA, JY-500RF). It is known that GD-OES analysis have features include are relatively simple experimental setup without the ultra-high vacuum technology, virtually no sample preparation, high speed of the analysis and the ability to analyze quantitative depth profiles of minor elements, with applications to diffusion phenomena in thin films or bulk materials[22].

3. RESULTS AND DISCUSSION

As demonstrated in Fig.4, the HA ceramics could be bonded to the Ti disks at the low temperature of 150°C using the above-mentioned HHP treatment. X-ray diffraction analysis had showed that the DCPD and $Ca(OH)_2$ powder materials were completely transformed into HA by the HHP treatment already[20].

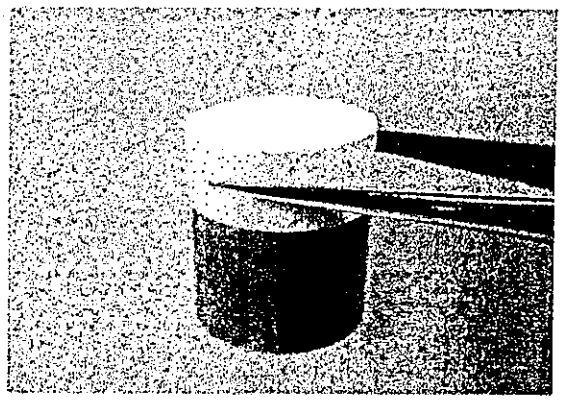

Fig.4 Photograph of the jointed body of HA ceramics and Ti.

Fig.5 shows a photograph of the fracture surface in the bonded HA/Ti body after 3-point bending test. It can be noted that the crack initiated from the pre-crack tip and propagated not along the HA/Ti interface, but into the HA. This observation suggests that the fracture toughness of the HA/Ti interface is close to or higher than that of the HA ceramics only. The critical stress intensity factor K_c was 0.30MPam$^{1/2}$ for the HA ceramics, and 0.28MPam$^{1/2}$ for the bonded HA/Ti. The toughness data are the average value obtained from at least five specimens. The K_c value for the bonded HA/Ti body gives a slightly lower value than that of the HA ceramics only. The difference in K_c data is potentially due to the residual stress induced by the thermal expansion mismatch between HA and Ti. The fracture appearance in Fig.5 may suggest that the interface toughness should be equal or higher than that of the HA ceramics only.

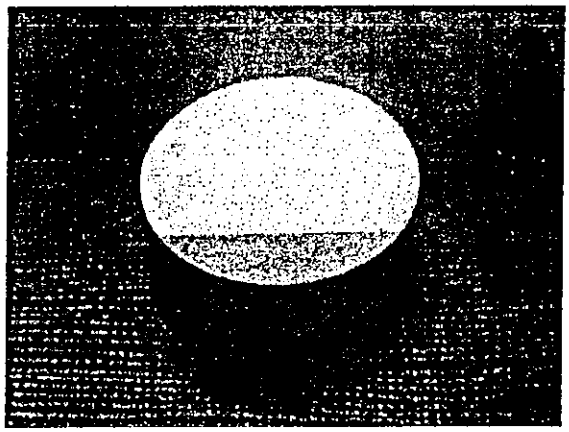

Fig.5 Photograph of fracture surface after 3-point bending test.

As shown in Fig.6, Depth profile of the chemical composition of Ti, Ca and O determined by GD-OES method indicated that the bonding of HA and Ti was achieved though the formation of a reaction layer at the HA/Ti interface. The thickness of the reaction layer was estimated to be approximate 1μm. Moreover, it was shown the elements of Ti and Ca were exchanged alternatively in HA ceramics. It seemed that the reaction layer and diffusion provided the bonding HA/Ti for absorbing the misfit between HA and Ti.

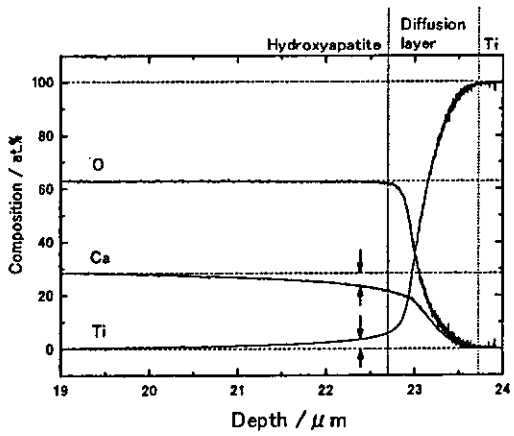

Fig.6 GD-OES analysis of the interface between the HA ceramics and Ti.

While further development is needed to improve the fracture property of the solidified HA, the HHP treatment may have the advantage over the plasma-spraying technique in the preparation of thermodynamically stable HA. The above results demonstrate the usefulness of the HHP method for bonding HA and Ti in order to produce a bioactive layer in biomaterials.

4. CONCLUSIONS

In this paper, it was demonstrated that HA could be bonded to Ti using a hydrothermal hot-pressing method at the low temperature of 150°C. The fracture toughness tests conducted on the bonded HA/Ti body revealed that the crack propagation from the pre-crack tip occurred not along the interface, but into the HA ceramics. The fracture toughness of the HA/Ti interface was also suggested to be close to or higher than that of the HA ceramics. This derived from the interface properties which HA and Ti changed the gradient within 1μm and which Ti and Ca were exchanged alternatively in HA ceramics.

ACKNOWLEDGEMENTS

This study was supported in part by the Japan Ministry of Health, Labour and Welfare under Grants-in Aid for Research on Advanced Medical Technology. Author T.O. was supported by research fellowship of the Japan society for the promotion of science for young scientists. Thanks are due to Mr. T. Nakamura of Horiba Company, Tokyo, Japan, for provision of time on a JY-500RF GD-OES instrument.

5. REFERENCES

(1) M. Long and H. J. Rack, *Biomaterials*, **19**, 1621 (1998).
(2) L. L. Hench, *J. Am. Ceram. Soc.* 81, 1705 (1998).
(3) M. Jarcho, J. F. Kay, K. I. Gummaer, R. H. Doremus and H. P. Drobeck, *J. Bioengng.* 1, 79 (1977).
(4) H. Aoki, "In Medical Applications of Hydroxyapatite", Ishiyaku Euro-America, Tokyo, Japan (1994), pp. 133- 154.
(5) J. G. J. Peelen, B. V. Rejda and K. De Groot, *Ceramurgia Int.* 4, 71 (1978).
(6) L. L. Hench, *J. Am. Ceram. Soc.* 74, 1487 (1991).
(7) P. Ducheyne, L. L. Hench, A. Kagan, M. Martens, A. Burssens and J. C. Mulier, *J. Biomed. Mater. Res.* 14, 225 (1980).
(8) S. R. Radin and P. Ducheyne, *J. Mater. Sci. Mater. Med.* 3, 33 (1992).
(9) K. De Groot, R. Geesink, C. P. A. T. Klein and P. Serekian, *J. Biomed. Mater. Res.* 21, 1375 (1987).
(10) X. Zheng, M. Huang and C. Ding, *Biomaterials* 21, 841 (2000)
(11) H. C. Gledhill, I.G. Turner and C. Doyle, *Biomaterials* 22,695 (2001).
(12) F. Fazan and P. M. Marquis, *J. Mater. Sci. Mater. Med.* 11, 787 (2000).
(13) K. A. Thomas, *Orthopaedics* 17, 267 (1994).
(14) E. E. Berry, *J. Inorg. Nucl. Chem.* 29, 317 (1967).
(15) A. Atkinson, P. A. Bradford and I. P. Selemes, *J. Appl. Chem. Biotechnol.* 23, 517 (1978).
(16) H. Monma and T. Kamiya, *J. Mater. Sci.* 22, 4247 (1987).
(17) T. Matsuno and M. Koishi, *Shikizai* 65, 238 (1992).
(18) N. Yamasaki, K. Yanagisawa, M. Nishioka and S. Kanahara, *J. Mater. Sci. Lett.* 5, 355 (1986).
(19) N. Yamasaki, T. Kai, M. Nishioka, K. Yanagisawa and K. Ioku, *J. Mater. Sci. Lett.* 9, 1150 (1990).
(20) K. Hosoi, T. Hashida, H. Takahashi, N. Yamasaki and T. Korenaga, *J. Am. Ceram. Soc.* 79, 2771 (1996).
(21) T. Hashida, *Int. J. Rock Mech. Min. Sci. Geomech. Abstr.* 30, 61 (1993).
(22) Z. Weiss and K. Marshall, *Thin Solid Films*, 308-309, 382 (1997).

(Received November 30, 2003; Accepted February 29, 2004)

北海道歯誌　25：330-338，2004.

原　著

各種顕微鏡および発光分光分析装置を用いた摘出インプラント周囲組織中のチタンの分析

横山　敦郎[1)]　松野　浩宜[2)]　川﨑　貴生[2)]　水越　孝典[3)]
石川　誠[4)]　戸塚　靖則[5)]　野田坂佳伸[6)]
宇尾　基弘[7)]　亘理　文夫[7)]　向後　隆男[8)]

抄　録：摘出インプラントについては，これまで主にインプラント周囲組織の組織学的検索やインプラント表面に対する走査型電子顕微鏡（SEM）を用いた研究がなされている．整形外科領域では，金属系生体材料の周囲組織の黒変現象であるメタローシスの臨床例が報告されているが，デンタルインプラントに関しての周囲組織の金属の分析はほとんどなされていない．本研究においては，摘出デンタルインプラント周囲組織内のチタンの分析を目的とし，SEMによる表面観察，組織学的検索に加え，走査型X線分析顕微鏡（XSAM）および発光分光分析装置（ICP）を用いて検索した．対象として，本学で施術し摘出したインプラントおよびその周囲組織に加え，他院で施術し本学で摘出したインプラントおよびその周囲組織を用いた．インプラント周囲組織に関してはパラフィン包埋し病理組織学的に検索するとともに，パラフィンブロックをXSAMにて分析した．また，周囲組織の一部を溶解し，ICPを用いてチタンを定量的に分析した．インプラントについてはSEM観察を行った．オッセオインテグレーションが成立せず補綴前に摘出したインプラントの周囲には，主に線維性結合組織が観察された．補綴後にオッセオインテグレーションを喪失し摘出したインプラントの周囲組織には，炎症性の円形細胞浸潤が散在性に観察され，一部に骨組織が認められた．XSAMを用いた蛍光X線分析にて，インプラント周囲組織に粒子状のチタンが検出された．ICPによる定量的分析でインプラント周囲組織には，3～30ppm程度のチタンが検出された．一部のインプラントでSEM観察によりチタンの剥離が認められた．以上の結果から，SEMや組織学的検索に加えXSAMおよびICPによる分析を行うことは，周囲組織のチタンの分布や定量を可能とし，摘出インプラント周囲組織のより詳細な解析に有効であることが示唆された．

キーワード：摘出インプラント，走査型X線分析顕微鏡，発光分光分析，チタン，オッセオインテグレーション

緒　　言

Brånemarkによるオッセオインテグレーションの概念の確立後[1)]，いわゆるオッセオインテグレーテッドインプラントは，歯牙欠損に対する補綴処置の一選択肢として広く普及してきている．臨床的に，無歯顎者へのデンタルインプラントの予後については20年以上の長期にわたる良好な予後が報告されており[2)]，現在では部分歯牙欠損や単独歯牙欠損に関しても優れた成績が報告されている[3-4)]．しかし，優れた予後に関する報告とともに，何らかの原因でオッセオインテグレーションが得られなかった，あるいは機能負荷後に喪失したという理由で摘出されたデンタルインプラントについての報告も数多くなされている[5-9)]．

近年，整形外科領域において，チタン製のプレートなど金属系生体材料を用いた際に周囲組織を黒変させる現象であるメタローシスが報告され[10-11)]，その原因としてフレッ

〒060-8586 札幌市北区北13条西７丁目
[1]北海道大学病院歯科診療センター咬合系歯科
[2]北海道大学大学院歯学研究科口腔機能学講座口腔機能補綴学教室
[4]北海道大学病院歯科診療センター口腔系歯科
[5]北海道大学大学院歯学研究科口腔病態学講座口腔顎顔面外科学教室
[6]北海道大学大学院歯学研究科中央研究部
[7]北海道大学大学院歯学研究科口腔健康科学講座生体理工学教室
[8]北海道大学大学院歯学研究科口腔病態学講座口腔病理病態学教室
〒003-8585 札幌市白石区東札幌３条３丁目
[3]東札幌病院歯科口腔外科
[受付：平成16年６月７日]［受理：平成16年７月12日］

ティングによる金属系生体材料からの摩耗粉の発生や材料表面からの金属イオンの溶出などが考えられている[11-12]．摩耗粉や金属イオンは，アレルギーやマクロファージの貪食による炎症などを惹起する可能性がある．また，チタンやチタン合金を使用した股関節形成術を受けた患者の血清のチタン濃度は高いという報告[13]や，動物埋入実験においてインプラント周囲や遠隔臓器にチタンが検出されたという報告もなされている[14-16]．デンタルインプラントについては，整形外科領域で使用される生体材料とは異なり，フレッティングなどの摩耗粉発生の要因は少ないものと考えられるが，手術操作における摩耗粉の発生の可能性は否定できず[12]，少数ではあるがメタローシスの報告もなされている[17]．このようなことから，デンタルインプラントについても，周囲組織中の金属の分析が必要と考えられる．しかし，摘出インプラントについての報告の多くはインプラントに対するSEM観察やその周囲組織に対する組織学的検索であり[5-9]，電子線マイクロアナライザ（EPMA）やX線マイクロアナライザー（EDX）を用いた摘出されたインプラント周囲組織の金属の分析に関する報告は少ない[18-19]．

周囲組織へのチタンの分散や溶出についての分析は，機能しているデンタルインプラントにおいては困難である．本研究では，種々の原因で摘出されたデンタルインプラントおよびその周囲組織を対象として，SEM観察や組織学的検索に加え，周囲組織中の金属を分析する目的で，EPMAやEDXに比較して前処理を必要とせず簡便な観察が可能であり生物試料の観察に有効であると考えられている走査型X線分析顕微鏡（XSAM）[20]を用いてチタンの分布を定性的に分析するとともに，発光分光分析（ICP）を用いてチタンの定量的分析を行った．

材料と方法

1．摘出インプラントについて

今回の検索症例の概要を表1に示す．本研究の対象とした摘出デンタルインプラントは9本で，4本は2次手術時あるいは補綴前にオッセオインテグレーションが得られなかったために摘出されたインプラントであり，5本は補綴後インプラント周囲炎によりオッセオインテグレーションを喪失し摘出されたものである．なお，本研究は北海道大学大学院歯学研究科・歯学部倫理委員会の承認を受けており，患者の同意を得た上で行われた．

2．検索方法について

摘出されたインプラントおよび周囲組織は10%中性ホルマリンにて固定後，インプラントと周囲組織を分離し，以下の検索を行った．

1）病理組織学的検索

インプラント周囲組織は二つに分割し，一片は通法に従いパラフィン包埋を行い，病理組織学的に検索した．

2）XSAMによる分析

包埋後のパラフィンブロックを対象として，XSAM（XGT-2000V　堀場製作所，京都）を用いて，チタン，カルシウム，イオウの各元素の面分析および点分析を行った．なお，X線導管（XGT）は，100μm径のものを使用した．面分析は3000秒/面の速度で25回積算し，点分析では各点300秒の測定を行った．

3）ICPによる分析

分割したインプラント周囲組織の一片を2N塩酸中で4時間煮沸後，希釈しICP発光分析装置（P-4010　日立製作所，東京）により，チタンの定量的分析を行った．

4）SEM観察

インプラントを対象として，SEM（S-4000日立製作所，東京）を用いて表面の性状を観察した．

結　果

1．病理組織学的検索について

オッセオインテグレーションが成立せず摘出された症例（Case 1）のインプラント周囲組織は，線維芽細胞および未分化な間葉細胞を含む線維性結合組織からなり，一部に径100μm程度の黒色の塊状の物質が観察された（図1－a）．一方，補綴処置後インプラント周囲炎によりオッセオインテグレーションが喪失し摘出された症例（Case 7および8）のインプラント周囲組織には，線維性結合組織内に黒色の塊状物質とともにリンパ球などの円形細胞浸潤や毛細血管の拡張などの炎症所見が認められた（図1－b，c）．インプラントの動揺により摘出された症例（Case 4）のインプラント周囲組織には，軽微な炎症反応が認められ，一部にインプラント体から離れて骨組織が観察された（図1－d）．

2．XSAMによる分析について

XSAMを用いて分析したインプラント周囲組織7例中4例に，チタンが明瞭に検出された（表2）．図2に

表1：検索症例の概要

Case No.	インプラントの種類	性別	摘出時年齢	埋入期間	機能負荷	摘出の原因
1	ブローネマルク	女性	56	7か月	−	オッセオインテグレーションの不成立
2	ブローネマルク	女性	56	7か月	−	オッセオインテグレーションの不成立
3	ブローネマルク	女性	56	7か月	−	オッセオインテグレーションの不成立
4	ブローネマルク	女性	60	7年	+	インプラントの動揺
5	アパセラム	女性	49	4か月	−	オッセオインテグレーションの不成立
6	アパセラム	女性	39	6年	+	インプラント周囲炎
7	ITI	女性	48	5年	+	インプラント周囲炎
8	インテグラル	女性	55	2年	+	インプラント周囲炎
9	ブレードタイプ	女性	49	5年	+	インプラント周囲炎

＊Case No1-3は，同一患者から摘出された

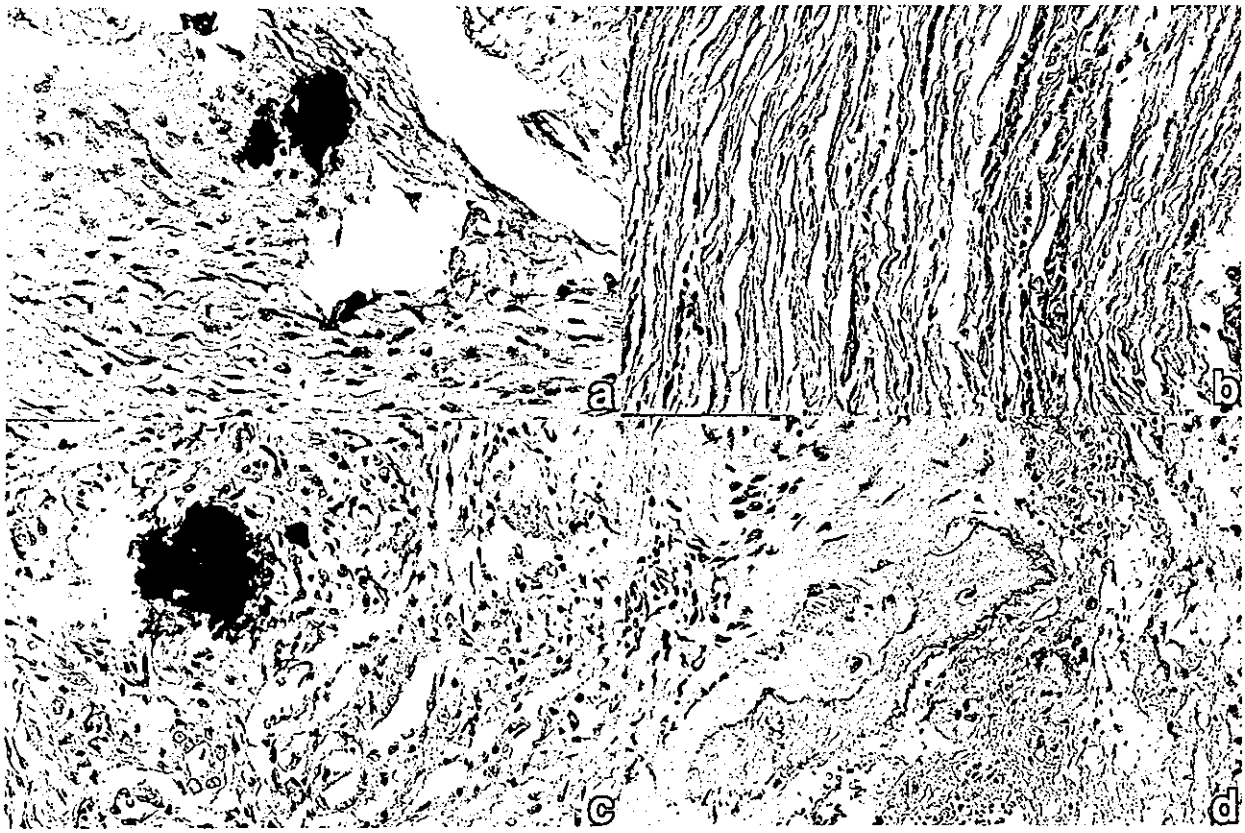

図1 摘出インプラント周囲組織の組織像
1－a：Case 1のインプラント周囲組織.黒色の粉状の塊周囲に未分化な間葉細胞や線維芽細胞に富む線維性結合組織が認められる．HE染色．原図100倍.
1－b：Case 8インプラント周囲組織．線維性結合組織中に軽度のリンパ球浸潤が認められる．HE染色．原図100倍.
1－c：Case 7インプラント周囲組織．黒色の粉状の塊周囲に拡張した毛細血管や炎症性細胞が認められる．HE染色．原図100倍.
1－d：Case 4インプラント周囲組織．肉芽組織中に骨組織が観察される．HE染色．原図100倍.

表2：摘出インプラント周囲組織のICPおよびXSAMによる分析結果

Case No	組織湿重量(mg)	Ti含有量(ppm)	XSAMでのTiの検出
1	15.0	30.0	+
2	21.9	15.5	*
3	24.0	5.4	±
4	10.2	10.1	+
5	21.0	3.8	*
6	46.1	17.0	±
7	10.1	20.1	+
8	26.2	5.0	±
9	60.0	22.0	+

*：XSAMで分析せず

XSAMによる面分析と点分析の結果の一部を示す．b，d，fのスペクトルは，a，c，eの矢頭で示した点における蛍光X線スペクトルである．図2－aは，Case 7のインプラント周囲組織のチタンの面分析であり，明瞭にチタンが検出された．図2－bに，チタンの点分析を示す．他の元素に比較しチタンの強度は著しい高値を示した．図2－cは，Case 8のインプラント周囲組織のチタンの面分析である．背景よりやや強い程度であり，点分析においても低い値を示した（図2－d）．組織学的検索において骨組織が認められたCase 4のインプラント周囲組織では，チタンとともにカルシウムが明瞭に検出された（図2－e，f）．

3．ICPによるチタンの定量的分析

表2にICP発光分析装置によるチタンの定量的分析結果を示す．対象としたすべてのインプラント周囲組織で3.8～30.0ppmのチタンが検出された．

4．SEM観察について

図3－aは，オッセオインテグレーションが成立しなかったため埋入4か月後に摘出された症例（Case 1）のインプラントの内ネジの表面であり，表面の一部に剥離が観察された．インプラント周囲炎のためオッセオインテグレーションを喪失し摘出されたインプラントでは，表面のコーティングの剥離や消失が観察された．Case 8のインプラントは，ハイドロキシアパタイトがプラズマ溶射されて

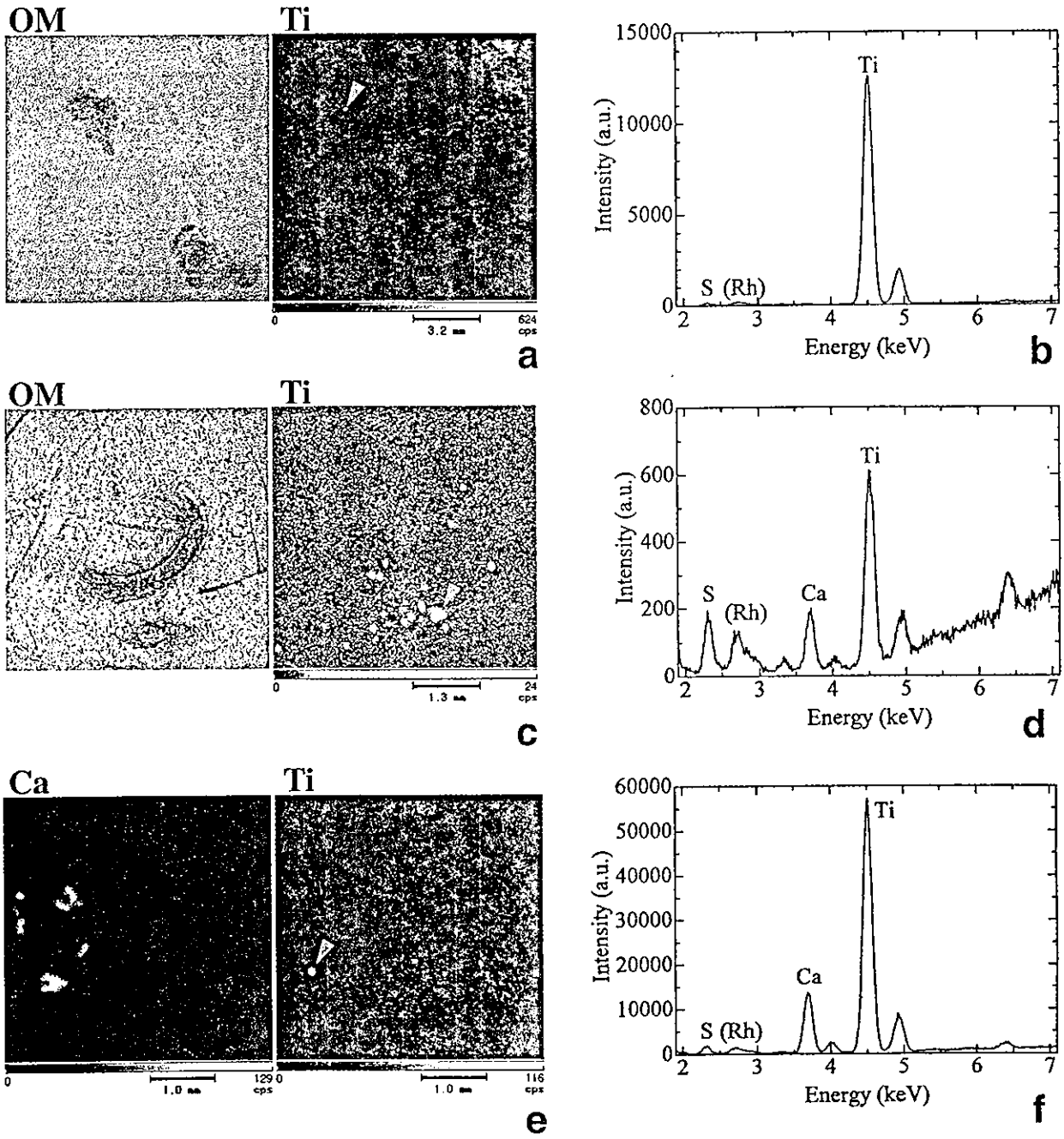

図2　摘出インプラント周囲組織のSXAMによる分析

2－a：Case 7インプラント周囲組織．OM：パラフィンブロック表面写真，Ti：XSAMによるチタンの面分析．灰色矢頭：検出されたチタン

2－b：2－a矢頭部の点分析．チタンの強度は高い．

2－c：Case 8インプラント周囲組織．OM：パラフィンブロック表面写真，Ti：XSAMによるチタンの面分析．背景に比較しやや強い白色の点が観察される．

2－d：2－c矢頭部の点分析．チタンの強度は，2－bに比較し著しく低い．

2－e：Case 4インプラント周囲組織．Ca：XSAMによるカルシウムによる面分析．Ti：XSAMによるチタンの面分析．

2－f：2－e矢頭部の点分析．チタンとカルシウムの検出強度は強い．

いたが，表面のコーティングされていたハイドロキシアパタイトは認められず，母材であるチタンが露出しており，インプラントの下端には桿菌と考えられる菌塊が認められた（図3－b，c）．Case 7のインプラント表面にはチタンがプラズマ溶射されていたが，チタンの一部の剥離・脱落が観察された（図3－d）．図3－eは，Case 4のインプラントの内ネジの表面である．図3－aと同種のインプラントであるが，埋入後7年を経過しており，インプラントの内ネジ表面には，ほぼ全体に鱗状の沈着物が観察された．

考　　察

1．XSAMおよびICPを用いた摘出インプラント周囲組織のチタンの分析について

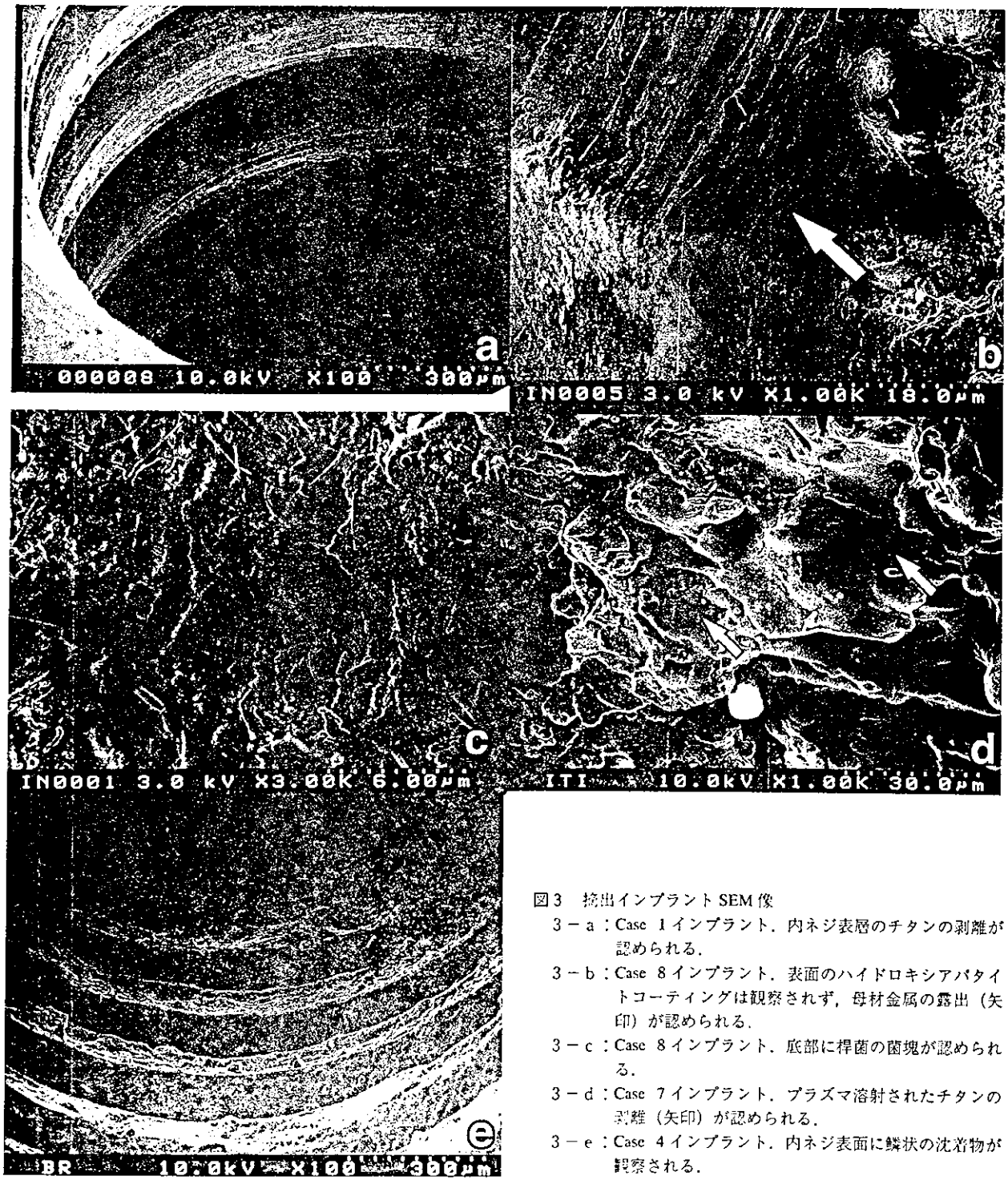

図3　摘出インプラントSEM像
3－a：Case 1インプラント．内ネジ表層のチタンの剥離が認められる．
3－b：Case 8インプラント．表面のハイドロキシアパタイトコーティングは観察されず，母材金属の露出（矢印）が認められる．
3－c：Case 8インプラント．底部に桿菌の菌塊が認められる．
3－d：Case 7インプラント．プラズマ溶射されたチタンの剥離（矢印）が認められる．
3－e：Case 4インプラント．内ネジ表面に鱗状の沈着物が観察される．

摘出インプラント周囲組織のチタンの分析に関する報告は少ない．Arys et al. は，XPS および EPMA を用いてオッセオインテグレーションが成立しなかったために摘出された11本のチタンインプラントについて分析し，わずか1本のインプラント周囲組織にチタンが検出されたとしているが，その検出限界によるものかもしれないと推察している[18]．本研究においては XSAM を用いて分析したが，7本中4本に明瞭にチタンを検出した．試料表層の約10nmを対象とする XPS や数μm の EPMA に比較し，XSAM は X線を試料に照射するため分析可能な深度は深く，このため周囲組織を一塊として検索することが可能で，周囲組織の一部にチタンが存在すれば検出できるものと考えられ，スクリーニングには有効な方法であることが明らかとなった．また，EPMA や EDS は，試料の損傷を防ぐために高度な前処置が必要であるが，XSAM は X線照射によるため試料への損傷が極めて少なく簡便に観察が可能であることが特徴であり[20]，量が限られる臨床試料の分析には適していると思われる．本研究においても Case 4のインプラント周囲組織で，チタンのみでなく，わずかな骨組織のカルシウムの検出が可能であった．Uo et al. は，ラット皮下組織に金属試料を埋入し，XSAM を利用して周囲組織の金属の溶出や濃度について詳細に分析し，その有効性を報告している[21-23]．

本研究において，XSAM により Case 1および7のインプラント周囲組織に，明瞭な点状のチタンが面分析にて確認され，点分析では著しい強度のチタンが検出された．この検出されたチタンは，面分析および点分析の結果から粉末状あるいは塊状のチタンであることが推察された．組織学的検索においても，これらのインプラント周囲組織には黒色の塊状構造が観察されたが，薄切，染色した標本については，XSAM では試料の厚みが不十分で十分な蛍光X線強度を得られないため，分析することが不可能で，チタンと同定することはできなかった．薄切した試料の分析には，むしろ EPMA や EDX が有効であると考えられる[18,19,24]．また，XSAM にて分析した7本中3本のインプラント周囲組織には，背景より若干高い程度のチタンが認められたが，検出誤差あるいはイオン化したチタンの可能性もあり，今後さらなる検討が必要であろう．

ICP による分析では，対象としたすべてのインプラント周囲組織にチタンが検出された．本方法では，イオン化していない粉状や塊状の固形のチタンに加えイオン化しているチタンも定量可能である．このため，XSAM では明瞭にチタンが検出されなかった周囲組織においても，チタンの検出が可能であったと推察された．

XSAM および ICP による分析で，インプラントの種類，埋入期間や炎症の有無などによるチタンの検出については，分析本数が少なかったため明らかな傾向は認められなかった．

2．デンタルインプラントにおける摩耗粉の発生について

デンタルインプラントでは，整形外科領域で使用されるインプラントに比較しフレッティングなどの要素は少なく，比較的摩耗粉の発生しにくい環境であると考えられるが，塙は，デンタルインプラントにおけるメタローシスについて，手術操作における摩耗粉の発生に言及している[12]．手術操作の他にも，対象としたインプラントのほとんどがアバットメントや補綴装置の連結にスクリューを用いており，摩耗粉の発生の一因となるものと考えられる．本研究において，XSAM による分析および組織学的検索により明らかとなった粉末状あるいは塊状のチタンは，SEM 観察により内ネジ表面のチタンの剥離やチタンコーティングの脱落により生じたことが示唆され，デンタルインプラントにおけるチタン摩耗粉の発生の可能性が示された．

3．オッセオインテグレーション不成立および喪失とインプラント周囲組織でのチタンの検出の関係について

Arys et al. はオッセオインテグレーションの不成立のため摘出されたデンタルインプラントを対象にインプラント表面を XPS で分析し，酸化チタン層の部分的な溶解や消失および周囲組織へのイオンの拡散がオッセオインテグレーションの不成立に関係しているのではないかと推察している[18]．Olmedo et al. は，摘出されたデンタルインプラント周囲でマクロファージがチタン粉を貪食していることを EDX で観察し，チタンの腐食がマクロファージを誘導し，サイトカインなどのケミカルメディエーターが破骨細胞を活性化し，骨吸収が生じ，オッセオインテグレーションの破壊につながると考察している[19]．一方，Ektessabi et al. はウサギの脛骨にチタンインプラント埋入し，micro ion PIXE を用いて分析し，オッセオインテグレーションが成立したインプラントの周囲組織，特に皮質骨でのチタンイオンの検出を報告し[25]，Ducheyne et al. は，イヌの海綿骨にチタンおよびチタン合金をインプラントし，インプラントに接する骨組織でのチタンイオンの検出を報告している[26]．本研究においては，メタローシスの臨床例のようにインプラント周囲全体に黒変した組織が認められないこと，XSAM による分析において摘出インプラント周囲組織にチタンの広範な分布が認められないことおよび病理組織学的検索において観察されたチタンと考えられる黒色の塊状物質は少量であり，マクロファージは少数であったことなどから，インプラントの摘出の原因が周囲組織において検出されたチタンと関係するとは現段階では考えにくい．臨床症例における血液や遠隔臓器での蓄積も含めデンタルインプラントからのチタンの摩耗粉の発生や溶出について，今後例数を増やすとともに，さらに EDX，EPMA や XPS などの分析機器を用いた詳細な検索が必要であろう．

結　　言

1．オッセオインテグレーションが成立しなかった，あるいは喪失したという理由で摘出されたインプラント周囲組織を分析したところ，剥離，摩耗したと考えられる固形チタンあるいはイオン化したと考えられるチタンが検出された．

2．XSAMおよびICPは，摘出したインプラント周囲組織のチタンの定性的および定量的分析に有効であることが示された．

文　　献

1）Brånemark,P.I., Hansson,B.O., Adell,R., Breine, U., Lindstrom, J., Hallen,O. and Ohman,A.: Osseointegrated dental implants in the treatment of the edentulous jaw. Experience from a 10-year period. Scand J Plast Reconstr Surg, **11**：1-132, 1977.

2）Ekelund, J.A., Lindquist, L.W., Carlsson, G.E. and Jemt, T.: Implant treatment in the edentulous mandible: a prospective study on Brånemark system implants over more than 20 years. Int J Prosthodont, **16**：602-608, 2003.

3）van Steenberghe, D., Lekholm, U., Bolender, C., Folmer, T., Henry, P., Herrmann, I., Higuchi, K., Laney, W., Linden, U. and Astrand, P.: Applicability of osseointegrated oral implants in the rehabilitation of partial edentulism: a prospective multicenter study on 558 fixtures. Int J Oral Maxillofac Implants, **5**：272-281, 1990.

4）Haas, R., Polak, C., Furhauser, R., Mailath-Pokorny, G., Dortbudak, O., and Watzek, G.: A long-term follow-up of 76 Brånemark single-tooth implants. Clin Oral Implants Res. **13**：38-43, 2002.

5）竹下文隆，松下恭之，黒木晴彦，山崎明美，末次恒夫：Hydroxyapatite coated blade implantの破折症例について　第1報：臨床例と組織学的観察．補綴誌　**38**：1102-1107, 1994.

6）Takeshita, F., Ayukawa, Y., Iyama, S., Suetugu, T. and Kido, M.: A histologic evaluation of retrieved hydroxyapatite-caoted blade-form implants using scanning electron, light, and confocal laser scanning microscopies. J Periodontol, **67**：1034-1040, 1996.

7）Eposito, M., Lausmaa, J., Hirsch, J.M. and Thomsen, P.: Surface analysis of failed oral titanium implants. J Biomed Mater Res (Appl Biomater) **48**：559-568, 1999.

8）Piatteli, A., Scarano, A., Piattelli, M., Vaia, E. and Matarasso, S.: A microscopical evaluation of 24 retrieved failed hollow implants. Biomaterials, **20**： 485-489, 1999.

9）高橋康則，永山正人，藤原秀光，三嶋　顕，青木秀希：HAコーティング層に結晶学的変化を認めた撤去症例．日口腔インプラント誌，**15**：216-222, 2002.

10）Matsuda, Y. and Yamamuro, T.: Metallosis due to abnormall abrasion of the femoral head in bipolar hip prosthesis. Impalnt retrieval and analysis in six cases. Med Prog Technol, **20**：185-189, 1994.

11）富田直秀：人工関節の劣化と生体への影響（メタローシスの成因と対策）．「生体用金属材料からの金属イオン溶出機構と人体への影響」研究会編，生体用金属材料からの金属イオン溶出機構と人体への影響，27-31，エリート印刷，つくば，1999.

12）塙　隆夫：インプラント表面と生体組織．上田実，赤川安正，市川哲雄，河野文昭編，先端医療シリーズ．歯科医学1歯科インプラント，57-63，先端医療技術研究所，東京，2000.

13）Jacobs, J.J., Skipor, A.K., Patterson, L.M., Hallab, N.J., Parposky, W.G., Black, J. and Galante, J.O.：Metal release in patients who have had a primary total hip arthroplasty. J. Bone and Joint Surg., **80-A**：1447-1458, 1998.

14）Bessho, K., Fujimura, K. and Iizuka, T.: Experimental long-term study of titanium ions eluted from pure titanium miniplates. J Biomed Mater Res. **29**：901-904, 1995.

15）Bianco, P.D., Ducheyne, P. and Cuckler, J.M.: Systemic titanium levels in rabbits with a titanium implant in the absence of wear. J. Mater. Sci. Mater. Med. **8**：525-529, 1997.

16）Jorgenson, D.S., Centeno, J.A., Mayer, M.H., Topper, M.J., Nossov, P.C., Mullick, F.G. and Manson, P.N.：Biologic response to passive dissolution of titanium craniofacial microplates. Biomaterials. **20**：675-682, 1999.

17）太田信知，藤本茂樹，田中克典，浅井澄人，下御領良二，大久保厚司，三島弘幸，小澤幸重：破折したITIインプラントの中空内骨に点在したTi合金粉の観察．第31回日本口腔インプラント学会学術大会抄録集．**145**：2001.

18）Arys, A., Philippart, C., Dourov, N., He, Y., Le, Q.T. and Pireaux, J.J.: Analysis of titanium dental implants after failure of osseointegration: Combined histologyical, electron microscopy, and X-ray Photoelectron Spectroscopy Approach. J Biomed Mater Res (Appl Biomater) **43**：300-312, 1998.

19）Olmedo,D., Fernandez, M. M., Guglielmotti, M.B. and Cabrini, R.L.: Macrophages related to Dental Implant Failure. Implant Dent.**12**：75-80, 2003.

20）宇尾基弘，亘理文夫：走査型X線分析顕微鏡による生物系試料の観察．北海道歯誌，**22**：61-63, 2001.

21）Uo, M., Watari, F., Yokoyama, A., Matsuno, H., and

Kawasaki, T.: Dissolution of nickel and tissue response observed by X-ray scanning analytical microscopy. Biomaterials **20**：747-755, 1999.

22) Uo, M., Watari, F., Yokoyama, A., Matsuno, H., and Kawasaki, T.: Tissue reaction around metal implants observed by X-ray scanning analytical microscopy. Biomaterials **22**：677-685, 2001.

23) Uo, M., Watari, F., Yokoyama, A., Matsuno, H., and Kawasaki, T.: Visualization and detectability of elements rarely contained in soft tissue by X-ray scanning analytical microscopy and electron-probe micro analysis. Biomaterials **22**：1787-1794, 2001.

24) 小林正義，渡辺孝一，宮川　修：波長分散型X線マイクロアナライザーにより生体組織切片の元素分布を得る試料作製法．新潟歯学会雑誌．**26**：29-37，1996.

25) Ektessabi, A.M., Ohtsuka, T., Tsuboi, Y., Yokoyama, K., Albrektsson, L., Sennerby, L., and Johansson, C.: Application of micro beam pixe to detection of titanium ion release from dental and orthopaedic implants. Int J PIXE, **4**：81-91, 1994.

26) Ducheyne, P., Willems, G., Martens, M., and Helsen, J.: In vivo metal-ion release from porous titanium-fiber material. J Biomed Mater Res. **18**：293-308, 1984.

Hokkaido J. Dent. Sci., 25 : 330-338, 2004.

ORIGINAL

Analysis of titanium in the tissue surrounding retrieved dental implants by microscopy and emission spectrochemical analysis

Atsuro Yokoyama[1], Hironobu Matsuno[2], Takao Kawasaki[2], Takanori Mizukoshi[3], Makoto Ishikawa[4], Yasunori Totsuka[5], Yoshinobu Nodasaka[6], Motohiro Uo[7], Fumio Watari[7] and Takao Kohgo[8]

ABSTRACT: Previously observations by scanning electron microscope (SEM) and histological evaluations have been mainly carried out for retrieved dental implants and the surrounding tissues. There are few studies of the analysis of metals in the tissue surrounding the retrieved dental implants, although clinical cases of metallosis have been reported in orthopedics. This study investigated titanium in the tissue surrounding retrieved implants by X-ray scanning analytical microscope (XSAM) and emission spectrochemical analysis (ICP) in addition to histological evaluations and observations by SEM. The retrieved dental implants and the surrounding tissue inserted at other dental clinics than Hokkaido University Hospital were used in the experiments. The histological evaluation and analysis by XSAM were done for the surrounding tissue. Titanium in the surrounding tissue was also analyzed quantitatively by ICP, and SEM observations were carried out on the retrieved implants. Fibrous connective tissue was mainly observed in the tissue surrounding the implants retrieved before prosthesis without formation of osseointegration. Non-continuous invasion of inflammatory round cells was observed in the tissue surrounding the retrieved implants after prosthesis by the destruction of osseointegration, while there was some bone tissue. Particles of titanium were detected in some of the surrounding tissue by XSAM; and 3-30ppm of titanium was detected in the surrounding tissue by ICP. Exfoliation of titanium from the inner thread of some of the implants was observed by SEM. These results suggest that analysis by XASM and ICP in addition to SEM and the histological evaluation are effective for the investigation of the tissue surrounding retrieved dental implants.

Key words: Retrieved dental implant, X-ray scanning analytical microscope, Emission spectrochemical analysis, Titanium, Osseointegration

[1]Department of Oral Rehabilitation, Center for Dental Clinics, Hokkaido University Hospital
[2]Department of Oral Functional Prosthodontics, Division of Oral Functional Science, Hokkaido University, Graduate School of Dental Medicine.
[4]Department of Oral and Maxillofacial Disorders, Center for Dental Clinics, Hokkaido University Hospital
[5]Department of Oral and Maxillofacial Surgery, Division of Oral Pathobiological Science, Hokkaido University, Graduate School of Dental Medicine.
[6]Central Research Division, Hokkaido University, Graduate School of Dental Medicine.
[7]Department of Biomedical, Dental Materials and Engineering, Division of Oral Health Science, Hokkaido University, Graduate School of Dental Medicine.
[8]Department of Oral Pathology and Biology, Division of Oral Pathobiological Science, Hokkaido University, Graduate School of Dental Medicine.
Kita13 Nishi7, Kita-ku, Sapporo, 060-8586
[3]Department of Oral Surgery, Higashi Sapporo Hospital
Higashisapporo 3-3, Shiroishi-ku, Sapporo, 003-8585
[Received: June 7, 2004] [Accepted: July 12, 2004]

Materials Transactions, Vol. 45, No. 11 (2004) pp. 3156 to 3162

Fabrication of Titanium Nitride/Apatite Functionally Graded Implants by Spark Plasma Sintering

Hideomi Kondo[1], Atsuro Yokoyama[1], Mamoru Omori[3], Akira Ohkubo[3], Toshio Hirai[4], Fumio Watari[2], Motohiro Uo[2] and Takao Kawasaki[1]

[1]*Removable Prosthodontics and Stomatognathostatic Rehabilitation, Department of Oral Functional Science, Graduate School of Dental Medicine, Hokkaido University, Sapporo 060-8586, Japan*
[2]*Dental Materials and Engineering, Department of Oral Health Science, Graduate School of Dental Medicine, Hokkaido University, Sapporo 060-8586, Japan*
[3]*Institute for Materials Research, Tohoku University, Sendai 980-8577, Japan*
[4]*Japan Fine Ceramics Center, Atsuta, Nagoya 456-8587, Japan*

Titanium nitride/hydroxyapatite functionally graded implant (TiN/HAP) was successfully fabricated by spark plasma sintering method (SPS) and their properties were investigated. The functionally graded materials (FGM) with the concentration from TiN at one end to HAP at the other were prepared by sintering at 1100 and 1200°C under the pressure of 150 MPa. The Brinell hardness was around H_B 60, nearly uniform for the whole range of composition. After 2 and 8 week implantation in diaphysis of femur of rat, there was very little inflammation and the new bone was formed around the sample. By use of TiN instead of Ti, the decomposition of HAP during sintering process could be suppressed and the successful sintering of FGM and mechanical properties could be attained.

(Received July 21, 2004; Accepted September 2, 2004)

Keywords: *titanium nitride, hydroxyapatite, functionally graded materials, spark plasma sintering, implant, biocompatibility*

1. Introduction

Pure titanium, titanium alloys, and hydroxyapatite are used for the implant in dental clinics as the method to restore the mastication function of lost teeth. Hydroxyapatite (HAP), a main component of bone and teeth, has bioactive properties for new bone formation.[1–3] Most of these implants are composed of the same structure and materials for the whole part. The dental implant needs the different function from part to part since it penetrates into a jawbone from the inside of the mouth. Inside the bone, the implant material is required to have osseoconductivity so that the new bone can be formed quickly and attached directly to it (osseointegration). In oral cavity (outside the bone), the implant material is required to have enough mechanical strength to bear the occlusal force. However, most of dental implants have the uniform composition throughout from the upper to bottom. The implant receives the force as much as 600 N at occlusion, nearly about the patient's weight. Inside jaw bone, the uniform fixation of the implant by new bone formation which completely surrounds the whole surface of implant is desirable to have the sufficient strength endurable to the occlusal force and to have the stress relaxation effect, that is, release of the excess overload on jaw bone. Dental implant with functionally graded structure would satisfy these requirements, high bone affinity and relaxation effect. Thus, we have been developing the dental implant where the concept of a functionally graded material (FGM) was applied. Figure 1 shows the concept of FGM implant. As a typical example, the left end is 100%Ti and the right end is 100%HAP. If Ti content increases, mechanical properties would be improved and as HAP content increases, biocompatibility could be improved.

Titanium/hydroxyapatite functionally graded implant (Ti/HAP) has thus been developed using pure titanium, titanium hydride, and surface nitrided titanium as the starting titanium materials for sintering.[4–16] However, HAP becomes unstable and decomposed under the coexistence of Ti which tends to act as reductant at high temperature. In Ti/HAP, the compromised optimum sintering temperature was found as 850°C where HAP is not decomposed.[15] However, at this temperature, sintering and mechanical intensity was insufficient. The use of more inert material, titanium nitride (TiN), would suppress the decomposition of HAP and enable the sintering at higher temperature. In this study, the TiN/HAP functionally graded implant was fabricated by Spark Plasma Sintering (SPS) and its mechanical properties and biocompatibility were investigated.

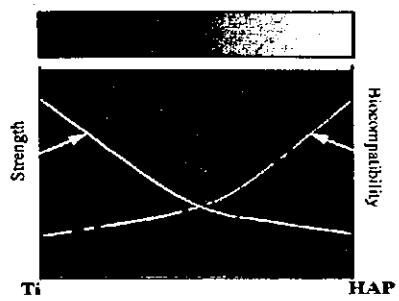

Fig. 1 Conception of FGM.

2. Materials and Methods

2.1 Preparation of FGM implant

The HAP powder which was crushed to pieces after sintered at 1150°C (SUMITOMO OSAKA CEMENT. <40 μm) and titanium nitride powder (NILACO Ltd.

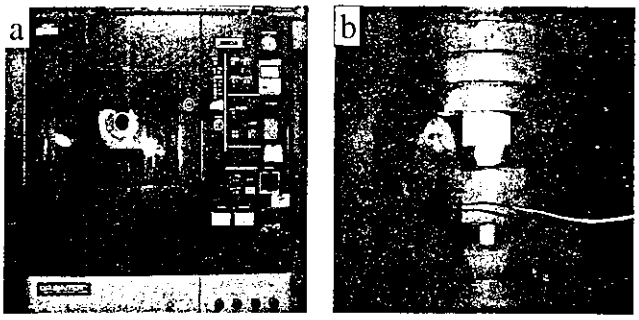

Fig. 2 a: Appearance of spark plasma sintering equipment. b: Sintering unit.

<45 μm) were blended with various ratios. These mixed powders with the different ratios of TiN and HAP were packed into the mold of ϕ20 mm × 10 mm, producing a gradient concentration from one end to the other to the depth direction. This TiN/HAP FGM was sintered under the pressure of 150 MPa at 900~1400°C by SPS. Figure 2 shows the appearance of SPS equipment. The sintered cylinder block was cut into the square rods for mechanical and animal implantation tests by the diamond disk, so that the composition gradient direction should be in the longitudinal axis.

2.2 Mechanical test

2.2.1 Brinell hardness test

The Brinell hardness test was performed in order to investigate the change of hardness in the direction of composition gradient. A steel ball with a diameter of 1.5 mm was indented under the load of 98 N for the loading time of 30 s. Three places were measured in each part of the eleven layers of gradient material, and their average was calculated.

2.2.2 Flexural test

The three point flexural test was done for the FGM rods (2 mm × 2 mm × 10 mm) with the gauge length of 10 mm and at the crosshead speed of 0.1 mm/min using the universal testing machine (INSTRON, Model 4204). Four specimens were tested and their average was calculated.

2.2.3 Compression test

The compression test was done for the FGM rods (3 mm × 3 mm × 7 mm) at the crosshead speed of 1 mm/min using the above universal testing machine. Four specimens were tested and their average was calculated.

2.3 Implantation test

Four Wister strain rats aged 14 weeks (weight 350~380 g) were used for the present experiments. After the rats were anesthetized with diethyl ether (Wako Pure Chemical Industries, Osaka Japan), pentobarbital sodium (30 mg/kg; EMBUTAL INJECTION, Dainabot, Osaka, Japan) was injected into the abdominal cavity of the rats. A hole was carefully made in the lateral surface of the diaphysis of femur using a dental round bur (ϕ1 mm), with a physiological saline external coolant, and the TiN/HAP FGM (1 mm × 1 mm × 7 mm) were inserted into bone marrow. The wound was then sutured. These rats were sacrificed at either the second or eighth week after implantation, and the tissue block involving specimens were resected. They were fixed in 10% neutral buffered formalin, washed, stained with Villanueva bone stain, and embedded in PMMA. After the tissue blocks were sectioned at 400 μm with a precision sawing machine (ISOMET 2000, BUEHLER, IL, USA), the thinner sections of about 100 μm in thickness were prepared by mechanical polishing.

2.4 Observation and analysis

Both FGM before implantation and in the tissue blocks involving specimens after implantation were observed and analyzed by optical microscopy (VANOX-S, OLYMPUS, Tokyo, Japan), SEM (HITACHI, S-2380N), electron probe micro analyzer (EPMA: JEOL JXA-8900M), and X-ray scanning analytical microscopy (XSAM: HORIBA, XGT2000V), and Raman spectroscopy (Dilor-Jobin Yvon-Spex-Horiba LABRAM).

3. Results

TiN/HAP FGM was fabricated by SPS at the temperatures 900~1400°C. For 900 and 1000°C the mechanical properties were insufficient to endure the mechanical shock at cutting process. For 1300 and 1400°C, the occurred after sintering, which was considered due to the decomposition of HAP.[15] The stable TiN/HAP FGM was obtained at 1100 and 1200°C.

Figure 3 shows the SEM observation of TiN/HAP sintered at 1100°C, the whole view (upper) and enlarged photographs of these parts (a: TiN b: 20HAP c: 80HAP d: 100HAP). The image of the part at high concentration of TiN (a, b) showed the porous structure and inadequate sintering. Sintering in the part at high concentration of HAP (c, d) was relatively more advanced and produced the condense structure.

Figure 4 shows the SEM observation of TiN/HAP sintered at 1200°C, the whole view and enlarged photographs of these parts (a: TiN b: 20HAP c: 80HAP d: 100HAP). Compared with the FGM sintered at 1100°C, sintering was advanced in each composition, although the sintering of 100%TiN region was still inadequate.

Figure 5 shows the Raman spectrum from 100%HAP region. The peak appeared near 3550 cm^{-1} is attributed to OH^-, which does not always appear in HAP. It suggests the attainment of good crystallinity.

Figure 6 shows the elemental mapping of TiN/HAP FGM by EPMA. Since Ca and P, the elements constituting HAP, show the same manner of distribution, it is suggested that HAP was not decomposed. It was also noted that Ti and N were similarly distributed in gradient and inversely to Ca and P in concentration, which proves the successfully prepared graded structure.

Figure 7 shows the Brinell hardness in each part of TiN/HAP FGM. The Brinell hardness was around 60, nearly uniform for the whole range of composition. There was not much difference between the FGM sintered at 1100 and 1200°C.

Figure 8 shows the flexural strength of TiN/HAP FGM. Flexural strength of the FGM sintered at 1100°C and 1200°C showed 65.4 MPa and 71.3 MPa, respectively. They were around the same level as a bone. The FGM fabricated at 900, 1000, 1300, and 1400°C was collapsed after sintering.

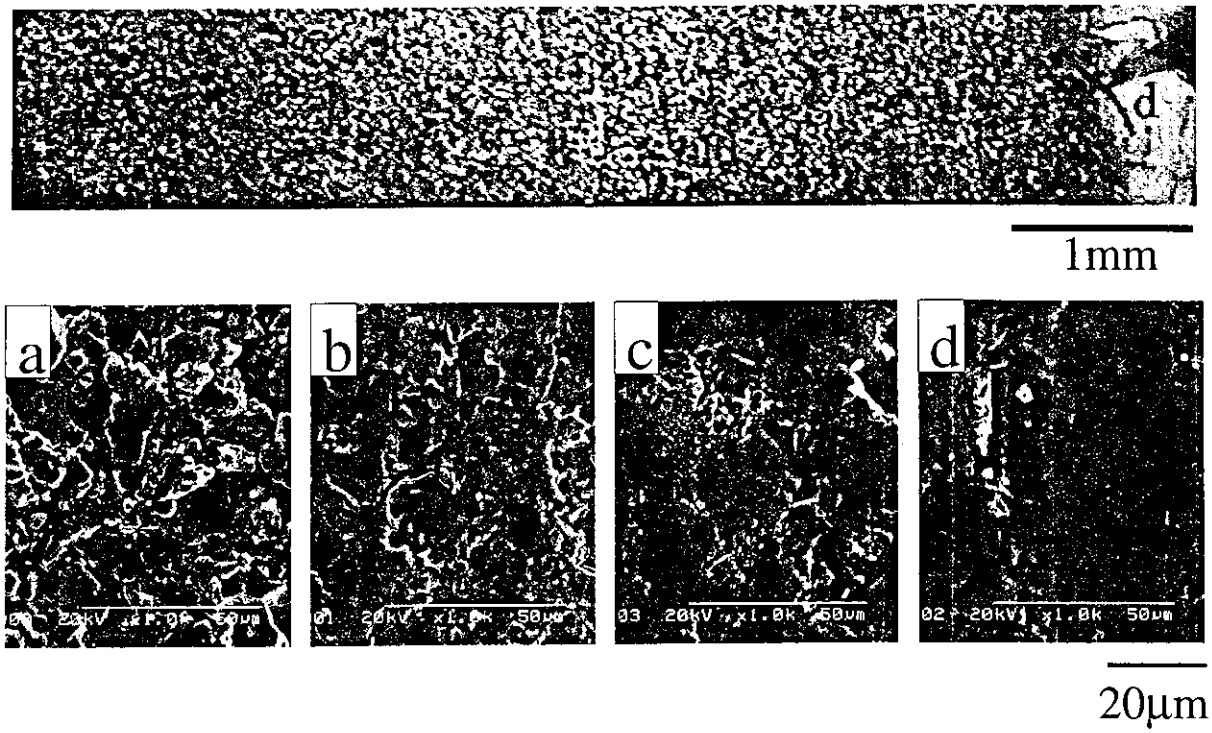

Fig. 3 SEM observation of TiN/HAP sintered at 1100°C. Whole view and enlarged photographs. a: TiN b: 20HAP c: 80HAP d: 100HAP.

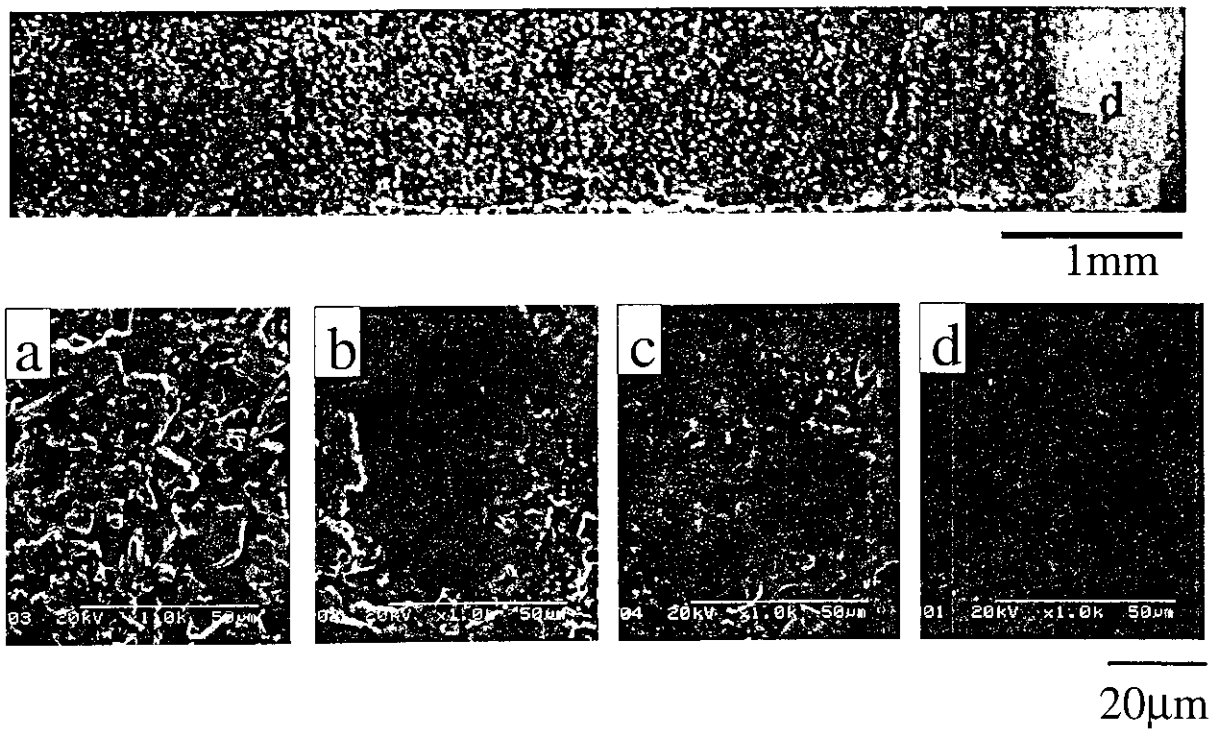

Fig. 4 SEM observation of TiN/HAP sintered at 1200°C. Whole view and enlarged photographs. a: TiN b: 20HAP c: 80HAP d: 100HAP.

Figure 9 shows the compression strength of TiN/HAP FGM. Both FGM showed the value larger than 100 MPa. The FGM fabricated at 900, 1000, 1300, and 1400°C was collapsed after sintering.

Figure 10 shows the light microscopic view of TiN/HAP implanted in the diaphysis of femur for 8 weeks in the transmission mode. Left side is 100%Ti and right side is 100%HAP regions. The cracks in 100%HAP were formed when the specimens were cut into slices for observation. The new bone was formed around FGM implant.

Figure 11 shows the enlarged views of newly formed bone in the regions of 90%TiN-10%HAP (a, c) and the 10%TiN-90%HAP (b, d) of TiN/HAP FGM after 2 and 8 weeks. The upper figures (a, b) show the newly formed bone around TiN/